

# PREFACE

This dissertation is submitted for the degree of Doctor of Philosophy at the University of Cambridge. The research described herein was conducted under the supervision of Professor H. K. D. H. Bhadeshia in the Department of Materials Science and Metallurgy, University of Cambridge, between October 1998 and October 2001.

This work is to the best of my knowledge original, except where acknowledgements and references are made to previous work. Neither this, nor any substantially similar dissertation has been or is being submitted for any other degree, diploma or other qualification at any other university. This dissertation contains less than 60,000 words.

Part of this work has been presented in the following publications:

T. Sourmail, *Precipitation in creep resistant austenitic stainless steels.*, Mat. Sci. Tech., 17:1, 1-14.

This was a highly commended entry of the Institute of Materials Literature Survey Competition 2001.

T. Sourmail, H. K. D. H. Bhadeshia and D. J. C. MacKay, *A neural network model of the creep strength of austenitic stainless steels.*, Mat. Sci. Tech., *in press*.

Thomas Sourmail

January 2002

## ACKNOWLEDGEMENTS

I would like to thank Professors D. J. Fray and A. H. Windle for the provision of the laboratory facilities in the Department of Materials Science and Metallurgy at the University of Cambridge. I am extremely grateful to my supervisor Professor H. K. D. H. Bhadeshia for his endless support, enthusiasm, knowledge and friendship.

I am indebted to Innogy Plc. and EPSRC for co-funding this project, and in particular to Dr David Gooch for his valuable comments and input throughout the project.

I would like to thank Hugh Davies and John Gisby from the National Physical Laboratory for their constant support with MT-DATA, together with the past and present members of the Phase Transformations and Complex Properties Research Group for their help and friendship, in particular to Harsha Sree Lalam, Miguel-Yescas Gonzales, Marimuthu Muruganath, Shingo Yamasaki, Catherine Neal, Gareth Hopkin, Hiroshi Matsuda, Pedro Rivera, Toshihiro Tsuchiyama, Franck Tancret, Pascal Jacques, Carlos Garcia, Daniel Gaude-Fugarolas.

Thanks also to my friends and to the people I met both at Darwin College and other Colleges during my time in Cambridge.

Finally, I take this opportunity to express my gratitude to my family for their love, unfailing encouragement and support.

# ABSTRACT

Despite their apparent simplicity due to their fully austenitic structure, modern Cr-Ni stainless steels are complex systems often containing more than 10 alloying elements. Offering excellent corrosion and creep resistance at elevated temperatures, they are choice materials for applications such as superheater tubes in steam power plants. Over the past 30 years, considerable improvement has been made to the strength of austenitic stainless steels, through careful chemical composition control and sometimes purposely designed heat-treatment.

The present work is concerned with the experimental study of the recently designed NF709, the best austenitic steel currently available on the market, and with the development of models to predict the microstructural evolution and mechanical properties of such steels. The experimental study of the precipitation state as a function of ageing time, which involves an array of complementary techniques, reveals precipitation sequences with no documented equivalent.

Physical modelling based on the theory for simultaneous transformations is used to attempt to predict the precipitation as a function of time. Full use of modern thermodynamic tools is made, avoiding previously necessary approximations. Once multicomponent effects are correctly accounted for, good agreement is obtained with published results. However, serious limitations are highlighted both in the absence of reliable quantitative experimental information, and in the lack of thermodynamic data on phases commonly found in modern austenitic steels.

A neural network in a Bayesian framework is used to estimate the creep strength and creep life of austenitic stainless steels. Models built with this technique not only reproduce correctly known influence of composition, but also grasp the interactions between different parameters. It is further shown to be a superior method of extrapolation when compared to conventional methods.

A new finding, that of  $\sigma$ -phase in a chromium-enriched NF709, is shown to be of no consequence to the long-term creep properties of the alloy.

# Contents

<b>1</b>	<b>Introduction</b>	<b>12</b>
1.1	Materials requirements in the power generation industry . . . . .	12
1.2	Austenitic stainless steels . . . . .	13
1.2.a	Composition and constituents . . . . .	13
1.2.b	Grades of austenitic stainless steels . . . . .	15
1.2.c	Modern grades for high-temperature applications . . . . .	18
<b>2</b>	<b>Precipitates in creep resistant austenitic stainless steels</b>	<b>21</b>
2.1	Carbides and nitrides in austenitic stainless steels . . . . .	21
2.1.a	MX precipitates . . . . .	21
2.1.b	Z-Phase . . . . .	26
2.1.c	$M_{23}C_6$ . . . . .	29
2.1.d	$M_6C$ . . . . .	35
2.2	Intermetallic phases . . . . .	39
2.2.a	Sigma phase . . . . .	39
2.2.b	Laves phase . . . . .	41
2.2.c	$\chi$ phase . . . . .	43
2.2.d	G-phase . . . . .	43
2.2.e	$Ni_3Ti$ and related precipitates . . . . .	46
2.3	Other precipitates . . . . .	47
2.3.a	$Cr_2N$ . . . . .	48
2.3.b	Pi-nitride . . . . .	48
2.3.c	Titanium carbosulphides . . . . .	48
2.3.d	Copper precipitates . . . . .	48
2.3.e	Chromium phosphides . . . . .	48

2.4	Concluding Remarks . . . . .	49
<b>3</b>	<b>Modelling precipitation reactions in steels</b>	<b>51</b>
3.1	Thermodynamic models for solution and compound phases . . . . .	51
3.1.a	Pure substances . . . . .	52
3.1.b	Random substitutional solutions . . . . .	52
3.1.c	Sublattice models . . . . .	54
3.1.d	The SGTE databases . . . . .	55
3.2	The classical theory for nucleation . . . . .	56
3.2.a	Nucleation rate in the classical theory . . . . .	56
3.2.b	Heterogeneous nucleation . . . . .	58
3.2.c	The driving force for nucleation . . . . .	59
3.3	The growth of precipitates . . . . .	60
3.3.a	Rate control . . . . .	60
3.3.b	Zener model for diffusion-control growth . . . . .	61
3.3.c	Capillarity effects on the interface compositions . . . . .	62
3.4	Overall transformation kinetics . . . . .	63
3.4.a	Soft-impingement . . . . .	64
3.4.b	Hard-impingement: the Avrami equation . . . . .	64
3.4.c	Modification for simultaneous reactions . . . . .	65
3.5	Summary . . . . .	66
<b>4</b>	<b>The growth rate of precipitates</b>	<b>67</b>
4.1	Introduction . . . . .	67
4.2	Calculation of the diffusion coefficients . . . . .	68
4.2.a	Calculation of the carbon diffusivity . . . . .	68
4.2.b	The diffusivity of Fe, Cr and Ni . . . . .	69
4.3	Calculation of the growth rate . . . . .	70
4.3.a	Calculating the growth rate in a binary system . . . . .	70
4.3.b	Calculation of the growth rate in a multicomponent alloy . . . . .	73
4.3.c	An algorithm to determine the tie-line satisfying the flux-balance . . . . .	75
4.4	Overall kinetics . . . . .	76
4.5	Consequences . . . . .	77

4.5.a	The growth rate . . . . .	77
4.5.b	The composition of $M_{23}C_6$ in the Fe-Cr-Ni-C system . . . . .	78
4.5.c	Number of components accounted for . . . . .	78
4.6	Comparisons and discussions . . . . .	79
4.7	Improvement in the calculation of the flux-balance tie-line . . . . .	80
4.8	Summary and conclusions . . . . .	82
<b>5</b>	<b>Capillarity in multicomponent systems</b>	<b>83</b>
5.1	Introduction . . . . .	83
5.2	Capillarity effects in a binary two phase system . . . . .	84
5.3	Ternary systems . . . . .	86
5.4	An exact calculation using MT-DATA . . . . .	88
5.5	Comparisons and comments . . . . .	91
5.5.a	The dilute solution approximation . . . . .	91
5.5.b	Effect of a Gibbs energy increase . . . . .	92
5.6	Consequences and conclusions . . . . .	93
5.6.a	Example . . . . .	93
5.6.b	Conclusions . . . . .	94
<b>6</b>	<b>Overall transformation kinetics</b>	<b>95</b>
6.1	Introduction . . . . .	95
6.2	Nucleation . . . . .	95
6.2.a	Calculating the driving force for nucleation . . . . .	96
6.2.b	The unknowns in the nucleation rate . . . . .	98
6.3	Overall transformation kinetics . . . . .	100
6.4	The tie-line shifting phenomenon . . . . .	101
6.5	Multiple precipitation reactions . . . . .	103
6.5.a	Precipitates drawing from the same solute . . . . .	103
6.5.b	Dissolution of precipitates and transient phases . . . . .	104
6.6	Predicting the behaviour of different steels. . . . .	106
6.6.a	The formation of $\sigma$ -phase in the AISI 300 series . . . . .	107
6.6.b	$\sigma$ -phase in AISI 304 . . . . .	107
6.6.c	Other steels in the AISI 300 series . . . . .	110

6.6.d	Other phases and difficulties . . . . .	115
6.7	Practical aspects of the software . . . . .	116
6.8	Summary and conclusions . . . . .	118
<b>7</b>	<b>Experimental Procedures</b>	<b>119</b>
7.1	Introduction . . . . .	119
7.2	Materials and heat-treatments . . . . .	120
7.3	Optical microscopy . . . . .	121
7.4	X-ray analysis of extraction residues . . . . .	121
7.5	Transmission electron microscopy . . . . .	123
7.5.a	Preparation of samples . . . . .	123
7.5.b	Identification of precipitates with TEM . . . . .	124
<b>8</b>	<b>Precipitation behaviour of NF709 and NF709R under static ageing at 750 °C and 800 °C</b>	<b>127</b>
8.1	Introduction . . . . .	127
8.2	Material and experimental procedures . . . . .	127
8.3	As-received material . . . . .	128
8.3.a	Prediction of the phases present in the as-received state . . . . .	128
8.4	Short term ageing . . . . .	132
8.4.a	TEM identification of the phases present in NF709 . . . . .	134
8.4.b	M <sub>23</sub> C <sub>6</sub> after very short ageing . . . . .	137
8.4.c	TEM identification of phases in NF709R . . . . .	137
8.5	NF709 aged 2500 and 5000 h at 750 and 800 °C . . . . .	139
8.6	NF709R aged 2500 and 5000 h at 750 and 800 °C . . . . .	142
8.7	Longer term ageing of NF709 and NF709R . . . . .	145
8.8	Summary and Discussion . . . . .	149
8.8.a	Summary . . . . .	149
8.8.b	Cr <sub>3</sub> Ni <sub>2</sub> SiN and G-phase in 20Cr/25Ni steels . . . . .	149
8.8.c	σ-phase formation and effect on mechanical properties . . . . .	151
8.8.d	Quantifying the precipitation . . . . .	154
8.9	Conclusion . . . . .	156

<b>9</b>	<b>Modelling the creep rupture life of austenitic stainless steels</b>	<b>157</b>
9.1	Neural Networks for empirical modelling . . . . .	157
9.1.a	The single neuron . . . . .	158
9.1.b	More complex networks . . . . .	158
9.1.c	Neural Network as a regression tool . . . . .	159
9.1.d	Learning and making predictions . . . . .	159
9.1.e	Practical aspects of the neural network training . . . . .	163
9.1.f	Committee Model . . . . .	164
9.2	Traditional empirical method for creep strength predictions . . . . .	166
9.3	Building a database . . . . .	167
9.4	Creep rupture life model . . . . .	169
9.5	Creep strength model . . . . .	173
9.6	Applications . . . . .	173
9.6.a	Molybdenum in AISI 304 and AISI 316 . . . . .	173
9.6.b	Chromium and boron . . . . .	174
9.6.c	The stabilisation ratio and solution temperature . . . . .	175
9.6.d	Comparison with other methods . . . . .	177
9.6.e	Software . . . . .	178
9.7	Summary and conclusions . . . . .	178
<b>10</b>	<b>Summary and future work</b>	<b>180</b>
	<b>APPENDIX ONE</b>	<b>182</b>
	<b>APPENDIX TWO</b>	<b>186</b>
	<b>APPENDIX THREE</b>	<b>190</b>
	<b>APPENDIX FOUR</b>	<b>192</b>



## Nomenclature and Abbreviations

$R$	the gas constant.
$P$	the pressure of the system.
$T$	the temperature of the system.
$t$	the time.
$G^0$	contribution of the pure components to the molar Gibbs energy of a phase indicated in subscript if necessary.
$G_{mix}^{id}$	ideal mixing contribution to the molar Gibbs energy of a phase indicated in subscript if necessary.
$G_{mix}^{xs}$	excess Gibbs energy change for mixing of a phase indicated in subscript if necessary.
$\varepsilon_{AB}$	the energy of a pair A-B.
$G_{\theta}^*$	the activation energy for homogeneous nucleation of phase $\theta$ .
$G_{d,\theta}^*$	the activation energy for nucleation on a dislocation.
$G_{B,\theta}^*$	the activation energy for nucleation on a grain boundary.
$G_t^*$	the activation energy for the transfer of an atom across the interface.
$x_i^{\gamma}$	the mole fraction of component $i$ in phase $\gamma$ .
$x_i^{\gamma\theta}$	the mole fraction of component $i$ in phase $\gamma$ in equilibrium with $\theta$ .
$\overline{x_i^{\gamma}}$	the average mole fraction of $i$ in phase $\gamma$ .
$y_i^k$	the site fraction occupancy of component $i$ on sublattice $k$ in a sublattice phase.
$\omega_{ij}^v$	the binary interaction parameter ( $i$ and $j$ ) in the Redlich-Kister development, depending on the value of $v$ .
$L_{A,B:C}$	the parameter for interactions between $A$ and $B$ on the first sublattice when $C$ occupies the second.
$G_{\theta}$	the molar Gibbs energy of phase $\theta$ .
$\Delta G_v$	the driving force for nucleation per unit volume of precipitate phase.
$\Delta G_n$	the driving force for nucleation per mole of precipitate phase.
$\Delta G_m$	the driving force for nucleation as defined by the parallel tangent construction.
$V_m^{\theta}$	the molar volume of phase $\theta$ .

$N_\theta$	the number density of nucleation sites for phase $\theta$ .
$N_v$	the number of atoms per unit volume.
$L_d$	the length of dislocation per unit volume.
$\sigma_{\gamma\gamma}$	the energy per unit area for an interface between the phases indicated in subscript.
$D_i^\gamma$	the volume diffusion coefficient of element $i$ in $\gamma$ .
$I_\theta$	the nucleation rate for phase $\theta$ .
$\psi_\theta$	the growth rate for phase $\theta$ .
$c_i^\gamma$	the concentration of component $i$ in phase $\gamma$ .
$c_i^{\theta\gamma}$	the concentration of component $i$ in phase $\theta$ in equilibrium with $\gamma$ .
$\bar{c}_i^\gamma$	the average concentration of component $i$ in phase $\gamma$ .
$\Omega_i$	the supersaturation of component $i$ .
$J_i$	the flux of component $i$ .
$\mu_{i,\theta}$	the chemical potential of component $i$ in phase $\theta$ .
$C$	shape factor relating the volume of a particle to the cube of its radius.
$V^e$	the extended volume of a phase indicated in subscript.
$V_p$	the volume of a particle at a given time.
$V_f(\text{phase})$	the volume fraction of a phase.
$V$	the total volume in which the transformation occurs.
$C_{Pi}$	the heat capacity for the temperature range $i$ .
$d_{hkl}$	the interplanar spacing for plans $(hkl)$ .
$\lambda$	the wavelength associated with electrons.
$\sigma$	the stress during a creep test.
$\sigma_{f,10^4h}$	the stress to obtain creep rupture after $10^4$ h.
$t_R$	the time to rupture.

TEM	Transmission Electron Microscopy.
SEM	Scanning Electron Microscopy.
EDX	Energy Dispersive X-ray analysis.
TTP	Time Temperature Precipitation.
MT-DATA	Metallurgical and Thermochemical Databank.
SGTE	Scientific Group Thermodata Europe.
JCPDS	Joint Committee of Power Diffraction Standard.
bcc	body-centred cubic.
fcc	face-centred cubic.
hcp	hexagonal close-packed.

# Chapter 1

## Introduction

The purpose of this chapter is to present the motivation for the research activities on creep-resistant austenitic stainless steels, and to provide a general background about these materials.

### 1.1 Materials requirements in the power generation industry

Over the last decade, considerable research has been devoted to the improvement of power plant efficiency. This is both for economical and environmental reasons: operating at higher temperatures improves the thermodynamic efficiency, and hence reduces the CO<sub>2</sub> emissions per unit of energy. In this context, materials-related issues are the limiting factor. Most of the steam-turbine plant now in service operate with a maximum steam temperature of 568 °C and pressure of 160 MPa, with the current state-of-the-art plant operating at 300 MPa, 600 °C [1]. When exposed for many years to such conditions, the tubes in which steam circulates have to offer suitable corrosion and creep resistance. Cost considerations imply that ferritic steels are used as much as possible, and considerable work is being devoted to design stronger ferritic alloys for use at operating temperatures of 650 °C. They also have a lower thermal expansion coefficient which makes them less prone to thermal fatigue.

However, the lower parts of the superheater tubes on a conventional boiler (figure 1.1), encounter temperatures at which ferritic steels cannot be used, and are therefore

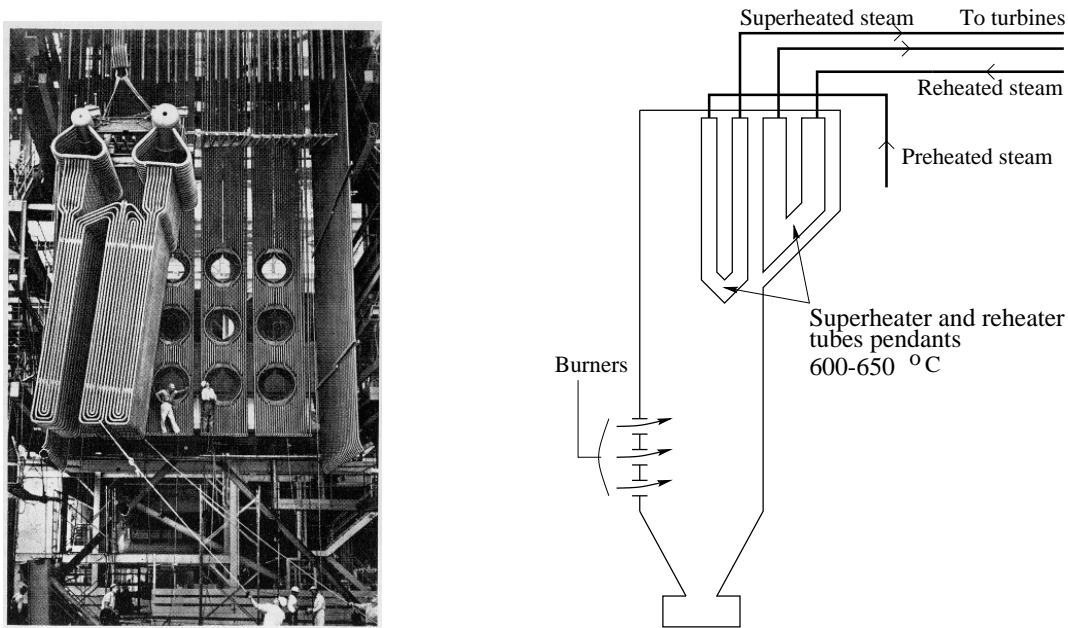


Figure 1.1: Superheater tubing (left) and scheme of a simplified boiler, after [2]

conventionally made out of austenitic stainless steels. As a part of the effort to improve the efficiency of power plants, much research focuses on improving the creep strength of these alloys, and consequently to raise their operating temperature.

The following gives a short introduction to the different austenitic stainless steels used in industry, and the latest compositions.

## 1.2 Austenitic stainless steels

### 1.2.a Composition and constituents

Austenitic stainless steels are essentially alloys of Fe-Cr-Ni, which owe their name to their room temperature austenitic structure. The addition of chromium has long been known to improve corrosion resistance. Chromium is also a 'ferrite stabiliser' and Fe-Cr stainless steels have a ferritic structure, possibly martensitic depending on the heat-treatment and exact chemical composition. The addition of austenite stabilising elements in sufficient quantities can allow an austenitic structure to be stable at all temperatures.

Nickel is the basic substitutional element used to stabilise austenite. The equilibrium phases depend on the proportion of the three elements, as well illustrated in an isothermal section of the ternary diagram for Fe-Cr-Ni (fig. 1.2) calculated using MT-DATA [3].

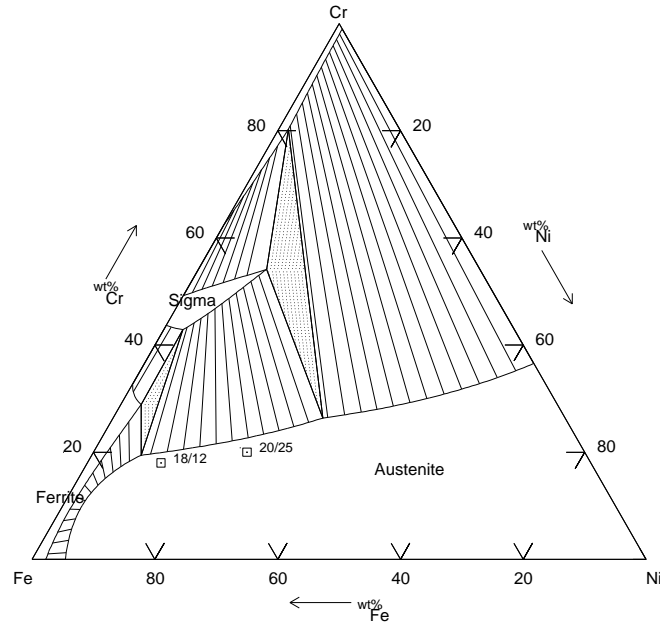


Figure 1.2: Isothermal section of the Fe-Cr-Ni diagram at 750 °C: a typical 18Cr-12Ni wt% lies in the austenitic field. Calculated using MT-DATA and the SGTE database.

Often, alloying elements, either interstitial such as C or N, or substitutional such as Mo, Mn, Ti, Nb, V, W, Cu, Al,... are also used to obtain the required properties. They can be classified as ferrite-stabilisers or austenite-stabilisers and their effect in this respect is often approximated using the notion of chromium and nickel equivalents, calculated by formulae like [4]:

$$\text{Ni}_{\text{eq}} = \text{Ni} + \text{Co} + 0.5(\text{Mn}) + 30(\text{C}) + 0.3(\text{Cu}) + 25(\text{N})$$

$$\text{Cr}_{\text{eq}} = \text{Cr} + 2.0(\text{Si}) + 1.5(\text{Mo}) + 5.5(\text{Al}) + 1.75(\text{Nb}) + 1.5(\text{Ti}) + 0.75(\text{W}) \text{ wt\%}$$

In this example, the composition has to be given in weight%. The use of such formulae is not always straightforward, as they rely on the austenite content, which can be modified by various precipitation reactions involving these elements.

Whether the austenitic structure is retained at room temperature depends on the  $M_S$  (martensite-start) temperature. Several empirical formulae have been derived to describe the effect of chemical composition on  $M_S$ , an example is [5]:

$$M_S(^{\circ}\text{C}) = 502 - 810(\text{C}) - 1230(\text{N}) - 13(\text{Mn}) - 30(\text{Ni}) - 12(\text{Cr}) - 54(\text{Cu}) - 6(\text{Mo}) \text{ wt}\%$$

A typical type 304 steel (table 1.2) has its  $M_S$  well below room temperature. However, it should be borne in mind that deformation-induced martensite formation can occur well above  $M_S$ .  $M_{d30}$  is the temperature at which 50% of martensite has formed for a true strain of 30%. Again, formulae like:

$$M_{d30}(^{\circ}\text{C}) = 497 - 462(\text{C} + \text{N}) - 9.2(\text{Si}) - 8.1(\text{Mn}) - 20(\text{Ni}) - 13.7(\text{Cr}) - 18.5(\text{Mo}) \text{ wt}\%$$

have been derived to describe the effect of alloying elements [5].

At high temperatures, a steel containing 18Cr, 12Ni wt% should be fully austenitic. However, the addition of other alloying elements often results in the formation of carbides, nitrides and intermetallics. These phases are not always desirable and a good knowledge of precipitation reactions is required to avoid loss of mechanical or chemical properties. A good example is the sensitisation of non-stabilised austenitic stainless steels: sensitisation occurs when the precipitate  $\text{M}_{23}\text{C}_6$  forms at grain boundaries, depleting the chromium content in the vicinity, which eventually results in intergranular corrosion. This can be avoided by tying up the carbon with strong carbide formers like Ti and Nb. The steel is then said to be stabilised. These precipitate phases will be described in detail in a later section.

### 1.2.b Grades of austenitic stainless steels

From a simple type 304 to the recent NF709, austenitic stainless steel compositions cover a large range. The two main alloying elements are chromium and nickel, so the steels will often be referred to by their content of Cr and Ni. For example, 18/10 refers to an austenitic stainless steels with 18Cr, 10Ni wt% .

**The AISI 300 series and other variants** The AISI 300 specifications for the compositions of different austenitic stainless steels (wt%) are shown in table 1.2 (after [6]).

wt%	C	Mn	P	Ni	Cr	
Type 304 [6]	≤ 0.07	≤ 2.00	0.04	8-10	17-19	
NF-709 [7]	0.06	1.00	0.006	25	20	
wt%	Mo	Nb	Ti	B	N	Si
Type 304	~ 0	~ 0	~ 0	~ 0	~ 0	~ 0
NF-709	1.5	0.26	0.05	0.005	0.167	0.40

Table 1.1: Compositions of two austenitic stainless steels

	C max.	Si max.	Mn max.	Cr	Ni	Mo	Ti	Nb	Al	V
<b>301</b>	0.15	1.00	2.00	16-18	6-8					
<b>302</b>	0.15	1.00	2.00	17-19	8-10					
<b>304</b>	0.08	1.00	2.00	18-20	8-12					
<b>310</b>	0.25	1.50	2.00	24-26	19-22					
<b>316</b>	0.08	1.00	2.00	16-18	10-14	2.0-3.0				
<b>321</b>	0.08	1.00	2.00	17-19	9-12		5×%C min.			
<b>347</b>	0.08	1.00	2.00	17-19	9-13			10×%C min.		
E 1250	0.1	0.5	6.0	15.0	10.0					0.25
20/25-Nb	0.05	1.0	1.0	20.0	25.0			0.7		
A 286	0.05	1.0	1.0	15.0	26.0	1.2	~1.9		~0.18	~0.25

Table 1.2: The AISI 300 series and other examples of heat resistant austenitic stainless steels; E1250 is Essete 1250. All compositions given in wt%.

Grades denoted L contain low carbon ( $< 0.03$  wt%) and ‘N’ contain nitrogen (eg: 316LN). Most often used as creep-resistant steels are types 316, 321 and 347, or alloys containing all of Mo, Nb and Ti. There are many other variants of these compositions, like the Japanese SUS300 series which mirrors the AISI 300 series, but sometimes with addition of both Ti and Nb. For convenience, as is sometimes done in the literature, the AISI 300 series will be used even for steels not strictly belonging to it, like a 316 with a Ti addition.

In fact, it is not the intention to describe, in the next chapter, the precipitation sequences in all different grades of creep-resistant austenitic stainless steels, but rather to examine the occurrence of the various precipitates in such a way that the precipitation behaviour of undocumented grades can be inferred from the conclusions reached.

There is a large amount of material on the precipitation phenomena in the 300 series of alloys, which have been used widely as creep-resistant steels. The same is true for 20Cr-25Ni steels. However, it appears that the long-term behaviour of Ti, Al alloyed austenitic stainless steels (type A286) is little documented [8]. This is possibly because production difficulties have restricted the application of such steels to parts requiring relatively small ingot sizes (aeroengine turbine discs), the design life of which is much shorter than the



few 100000 h required for steam plants [9].

### Role of alloying elements

- Mn has been introduced in austenitic stainless steels as a substitute for Ni during shortages in the international market or for economical reasons. The nickel content can be halved to 4 wt% by the addition of 2-6 Mn wt%. Although the austenitic structure is achieved, such steels do not exhibit the same corrosion resistance as an 18/8 steel. Mn is also used to increase the solubility of nitrogen in austenite.
- Mo is, on the contrary, a ferrite stabiliser. It improves the creep properties of stainless steels by solid solution hardening and also improves the resistance to pitting corrosion. It also facilitates carbides precipitation. However, it promotes  $\sigma$ -phase and Laves phase formation on long term ageing.
- Stabilising elements like niobium, titanium and vanadium greatly improve the creep strength of austenitic stainless steels mainly by precipitating fine carbides intragranularly. On the other hand, they reduce the creep ductility. The ratio in which they are added to carbon is important to maximise the strengthening effect and avoid precipitation of detrimental phases. They can also have a solid-solution strengthening effect.
- Carbon acts principally by solid-solution strengthening in non-stabilised grades, but mainly by precipitation strengthening when Nb, Ti or V are present.
- Nitrogen is a strong austenite stabiliser. It has also a role in increasing the creep life of austenitic stainless steels: it can act like carbon in stabilised stainless steels by precipitating in the form of titanium or niobium nitrides, but the nitrogen remaining in solid solution has also a much greater strengthening effect than carbon. It has been believed to lower the diffusivity of chromium and carbon in the matrix, therefore delaying the coarsening of precipitates [5, 6]. However, more recent results indicate that nitrogen enhances chromium diffusion, but retards the nucleation of  $M_{23}C_6$  because of its low solubility in this carbide [10].

### 1.2.c Modern grades for high-temperature applications

Steels from the AISI 300 series have been used for long in power plant, where strong corrosion resistance and creep strength are required. Modern austenitic grades have however significantly improved over these by the use of new combinations of chemical elements, such as SUPER304H which, in addition to the required composition of a 304 steel, contains Nb, N and Cu; SAVE25 which contains W, Nb, Cu and N, or NF709, presented previously.

Figure 1.3 illustrates the development progress of austenitic steels for boilers, and on the far right, the most advanced austenitic stainless steels, which all contain several other elements in addition to Cr and Ni. In practice, the compositions are controlled much more accurately than suggested by the intervals of compositions and include controlled additions of B which has been shown to have beneficial effects on the creep strength.

Figures 1.4 and 1.5, adapted from [11], compare the allowable stresses as a function of temperature, for some of these steels, and give a clear idea of the progress that has been made from the H-Grade AISI 300 series. The definition of ‘allowable stress’ is not given in this reference; the value of the stress probably refers to a particular service life.

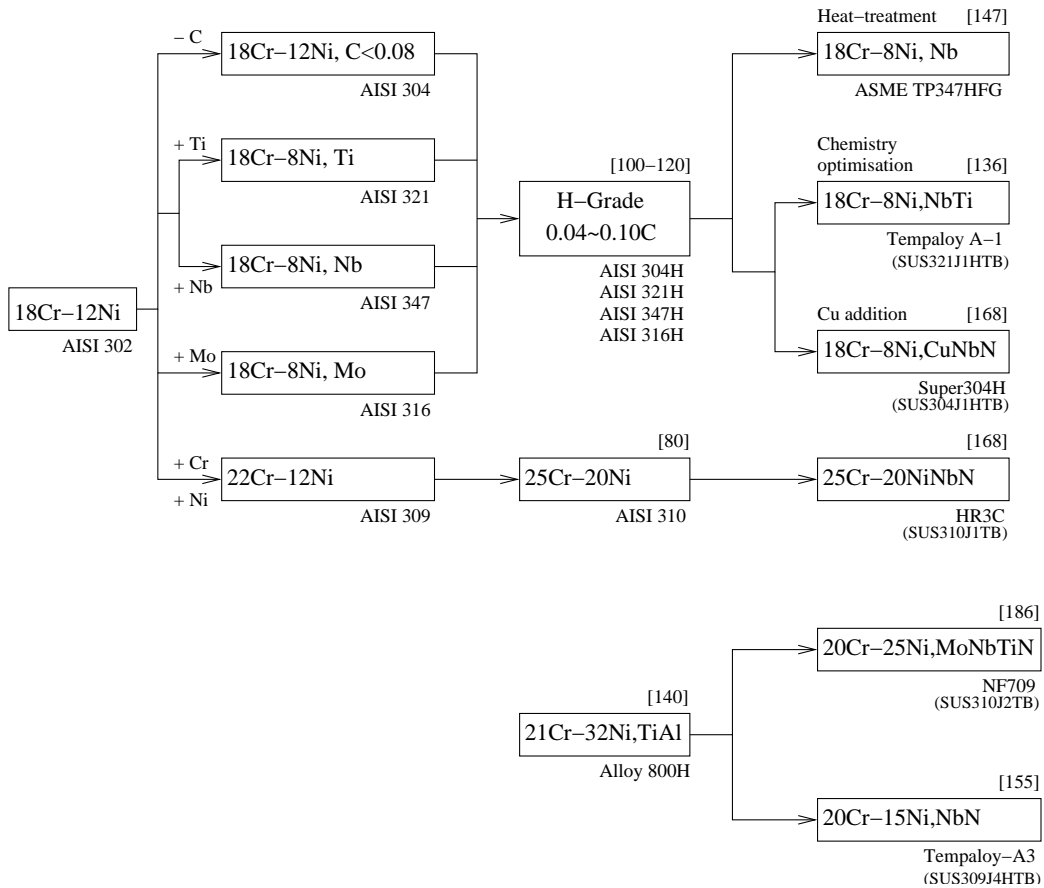


Figure 1.3: The development progress of austenitic stainless steels for high temperature applications, after [11]. Numbers in square brackets indicate the  $10^5$  h creep rupture strength at 600 °C.

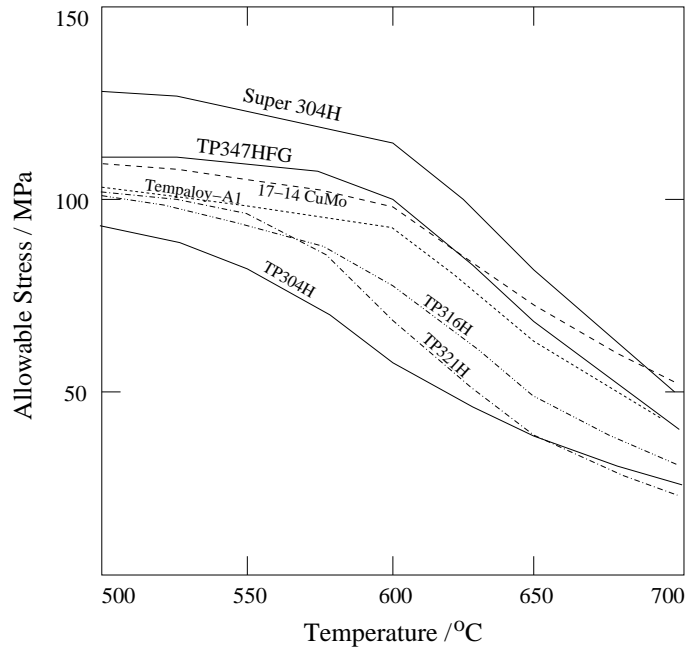


Figure 1.4: The allowable stresses for some austenitic stainless steels for high temperature applications, based on 18Cr-8Ni or 15Cr-15Ni steels. After [11].

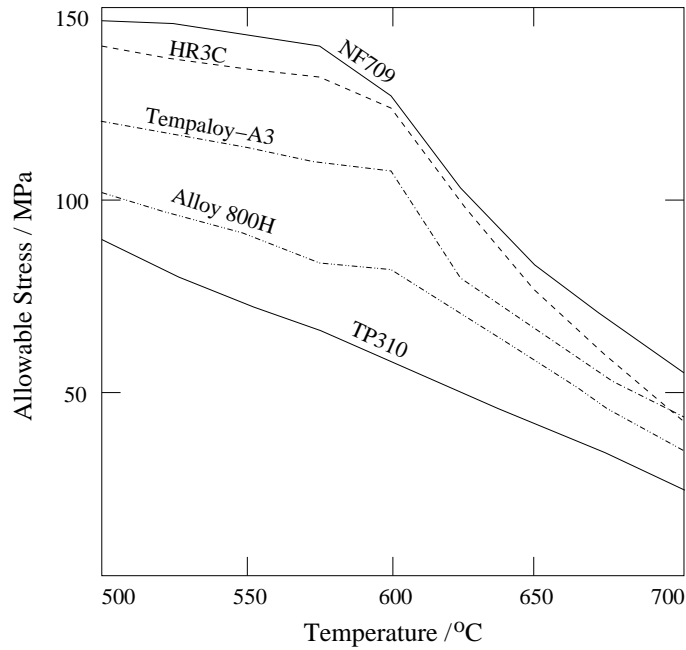


Figure 1.5: The allowable stresses for some austenitic stainless steels for high temperature applications, based on 20Cr-25Ni or other high-Cr, high-Ni steels. After [11].